Inter-cell Interference for Reverse Link in WCDMA

LAURA GARCIA-LOPEZ[1], MARIO REYES-AYALA[2], SERGIO VIDAL-BELTRAN[1]
[1]National Polytechnique Institute
ESIME, Research and Postgraduate Studies Section
Av. IPN , Z-4 Tower, 3rd Floor, Col. Lindavista, Zip Code 07738 Mexico City
MEXICO
[2]Electronics Department
Metropolitan Autonomous University
San Pablo 180, Col. Reynosa Tamaulipas, Azcapotzalco, ZIP Code 02200, Mexico City
MEXICO
mra@correo.azc.uam.mx

Abstract: - In this paper, the WCDMA inter-cell interference is carried-out for both, soft and hard handovers. The main parameters used to evaluate the proposed model were the other-cell interference factor and the outage probability. The results of this work allow us to compare any sort of frequency reuse schemes in this spread-spectrum multiple access technique.

Key-words: - soft HO, hard HO, frequency reuse scheme, fading, inter-cell interference, WCDMA.

1 Introduction

The personal communications systems PCS are based on three techniques: Frequency Division Multiple Access (FDMA), Time Division Multiple Access (TDMA) and Code Division Multiple Access (CDMA). The CDMA has some advantages: security, a lot of simultaneous users, intentional interference cancellation and a large bit rate. In this paper, a variety of CDMA named Wide-CDMA (WCDMA) is analyzed, when a user is in the cell boundary.

WCDMA has been adopted by the most important PCS technology 3GPP (Third Generation Partnership Project). It is very common to identify this standard as UTRA (Universal Terrestrial Radio Access) [1] [2] [3].

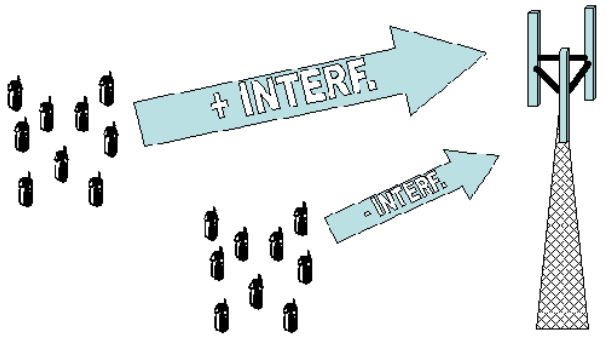

Fig. 1 Near-far effect

In a cellular system, the capacity is determined by the near-far effect, because the nearest terminal can block the base station. The signal strength of the nearest users is notably greater than the other users. At the same time, the intentional interference caused by other base stations is lower in the users close to the reference base station. In the Figure 1, this effect is illustrated.

As a consequence of near-far effect, it is very important to use a power control algorithm to optimize the system capacity. One of the most important part of this algorithm is the call transfer strategy. This procedure is frequently named handover.

In this article, the performance handover is calculated, hard and soft variations are taking in account for the most important frequency reuse schemes.

The paper is organized in five sections, section one is dedicated to a introduction, in section two the WCDMA technique is presented, in section three the empirical propagation model is analyzed, in section four the handover mechanism and its variations are presented, in section five the main results of this work are shown and, the section six are the conclusions.

2 Propagation Model

The multipath radio wave propagation involves the transmitted signal spreading. The presence of many

objects and obstacles may cause diffraction, reflection and refraction. The superposition of these waves sometimes produces a composed signal with some spread parameters: delay, phase, amplitude and polarization.

The large and far objects cause long-term variations and slow (log-normal) fading. The near obstacles create rapid short-term variations and fast (Rayleigh) fading.

The scattering process in mobile radio channels can be modeled as a Wide Sense Stationary Process [13]. The mobility of the terminal equipment is limited by the Doppler effect, because the relative velocity of the users generates a carrier frequency variation [14]. In this case, the channel can be modeled as a filter, where linear distortion is evaluated [15].

The propagation model used in this article is determined by equation 1.

$$10\log_{10}\alpha(r,\zeta) = 10\mu\log_{10} r + \zeta \qquad (1)$$

Where:

α Attenuation, dB.
γ Required margin, dB.
σ standard deviation of ζ.
ζ log-normal shadowing.
μ power of distance.
r Distance from a base station, m.

Experimental results give us the most common values in this model are: $\sigma = 8$ and $\mu = 4$, [1] [2] [3] [8].

The model proposed in this work assumes a lo-normal fading only, because in the city the signal has normally this behavior.

3 WCDMA

In WCDMA systems, the performance can be increased for very wide spread bandwidth. But, this feature face the implementation challenge, because the receivers must be design to operate in the conditions mentioned before [11].

In the Table 1 the main parameters of WCDMA are listed.

Carrier Separation	5 MHz
Chip rate	3.84 Mcps
Frame duration	10 ms (38400 *chips*)
Number of bursts in the frame	15
Number of chip per burst	2560 chips
Number of bursts in the uplink	4 a 256
Number of bursts in the downlink	4 a 512
Bit rate in the channel	7.5 kbps a 960 kbps

Table. 1 WCDMA features

The Core Network (CN) of the WCDMA may change to the Global System for Mobile Communicatrions (GSM). The general architecture includes two main parts: the user terminal (Terminal equipment and Mobile Termination) and the physical nodes. In the Figure 2, the Universal Mobile Telecommunications System (UMTS) architecture is shown.

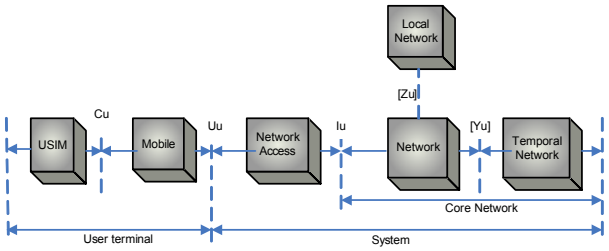

Fig. 2 UMTS Architecture

The network elements are grouped in the Radio Access Network (RAN). This part of the network manage the functions related to the radio access. The core network is dedicated to the call switching and routing.

The Figure 3 shows the architecture of the UTRAN system.

The base station (Node B) has the following main tasks: channel coding, modulation and spreading. The RNC is the Radio Network Controller and coordinates the operation of several base stations. The MSC/VLR and SGSN provide the base for circuit-switched and packet-switched networks respectively. Then SGSN is related with the General Packet Radio Services (GPRS).

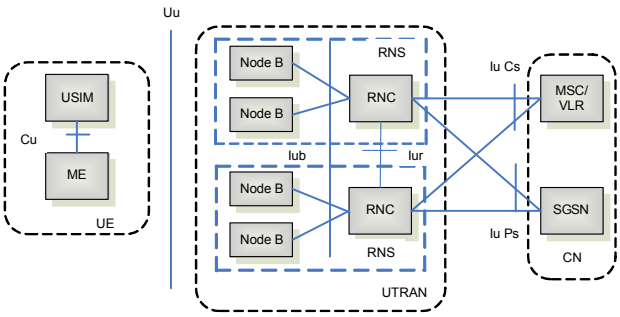

Fig. 3 UTRAN Architecture

There are three layers in the WCDMA system: logic channels (describe the kind of data to be transmitted), transport channels (indicate the logic channels transfers) and physical layers (give the radio environment). The Figure 4 illustrates the channels of WCDMA.

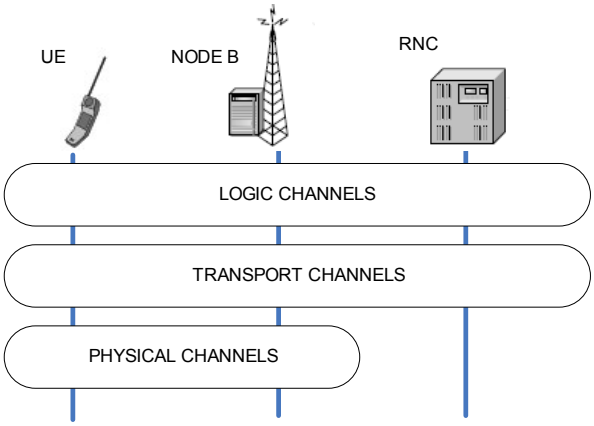

Fig. 4 WCDMA Channels.

WCDMA has a frame structure divided by 15 burst (slot time). The figure 5 shows the burst distribution in the WCDMA frame.

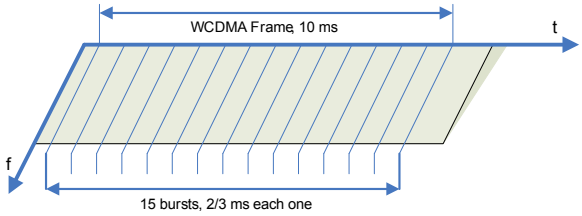

Fig. 5 WCDMA Frame.

The figures 6 show the up-link of the dedicated channel. This channel has user and signaling information, it is needed to assure the bit rate.

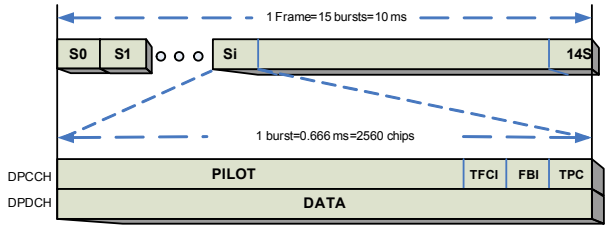

Fig. 6 Frame of Physical Channel (up-link).

The frames are marked by the Frame Number System (SFN). This system is internally used to synchronize the UTRAN and the transmission timing.

In the Figure 7, the frame of physical channel for the reverse channel is illustrated. It is very important to highlight the pilot position in this down-link frame.

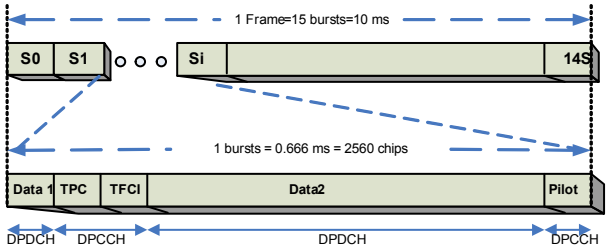

Fig. 7 Frame of Physical Channel (down-link).

In the real-world handset operations in the WCDMA system, the mobile requires a very high clock stability, because the spreading PN-sequences must be synchronized in the mobile and base stations equipment [8].

The antennas considered in the model are the ideal monopoles with omni-directional radiation patterns. The model can be enhanced including flared monopole antennas [10].

The bit error rate of the WCDMA systems depends on a lot of parameters. In this paper, the other-cell interference factor is widely evaluated, in order to compare with the average signal power. Other parameters can be taken in account [12].

4 Handover in WCDMA

In order to assure mobility in a PCS network, it is necessary to make call transfers (handover or handoff). There are three ways to do the handover (HO), and the decision is taken by the signal power level of the terminal equipment.

The strategies mentioned above to get handover or handoff are: hard handover (Hard HO), soft handover (Soft HO) and softer handover.

In the Figure 8 the Handover procedure is illustrated. The measurement implies the inter-cell inteference in the reverse link, because the forward link requires no power control mechanism, since the base station transmits all the signal together.

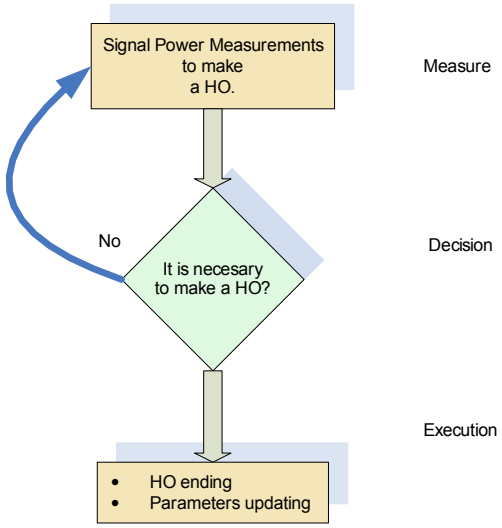

Fig. 8 Handover steps.

In Hard HO there is a very short pause, because it is necessary to finish a communication before the beginning of a new communication [1] [3] [5]. The users can not detect the pause.

The soft HO technique implies two communications links in separate cells, then, there is not a pause. The softer strategies involve sectorization of the cell and two communication between separate sectors. The soft HO is mainly employed in packet- switched network. The RNC play a pivotal role providing the connection between base stations involved in the procedure. The serving RNC combines the received signals and sends them to the MSC/VLR.

The quality of service in this kind of system is determined by the probability of a poor signal to interference ratio, this parameter is the outage probability.

In the case of Hard HO, this condition can be calculated by equation 2.

$$P_{out} = \Pr(\zeta < \gamma) = \frac{1}{\sqrt{2\pi\sigma}} \int_{\gamma}^{\infty} e^{-\zeta^2/2\sigma^2} d\zeta = Q\left(\frac{\gamma}{\sigma}\right) \quad (2)$$

Where:

Q Marcum-Q function.
P_{out} Outage probability.
ζ Log-normal distributed shadow effect, dB.
σ Standard deviation of the shadowing, dB.
γ Margin, dB.

It is obvious that the ideal Hard HO may produce a lot of call transfers. This problem is known as ping-pong effect. The easiest solution to this, is to require a sufficient amount of signal power reduction, in comparison with the other base station.

The Figure 9 shows the outage probability in comparison to distance from base station. In this case the worst case is equal to 10%.

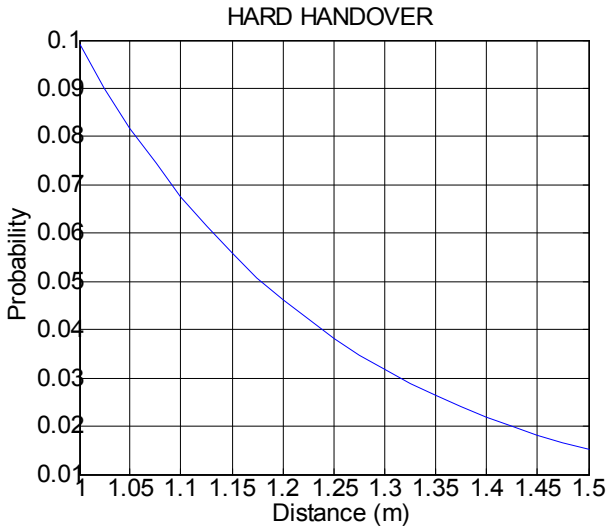

Fig. 9 Hard HO.

In Soft HO the margin is selected from two margins: the nearest cells. Then the outage probability is calculated by equation 3.

$$P_{out} = \frac{1}{\sqrt{2\pi}} \int_{-\infty}^{\infty} e^{x^2/2} \left[Q\left(\frac{\gamma + a\sigma x}{b\sigma} \right) \right]^2 dx \quad (3)$$

Where:

Q Marcum-Q function.
P_{out} Outage probability.
a, b Geometric constants.

It is necessary to consider that the soft HO requires the resources of two or more base stations. In addition to this, the interference power level is also increased at the boundary of the cell.

The performance of this sort of handover is plotted in Figure 10.

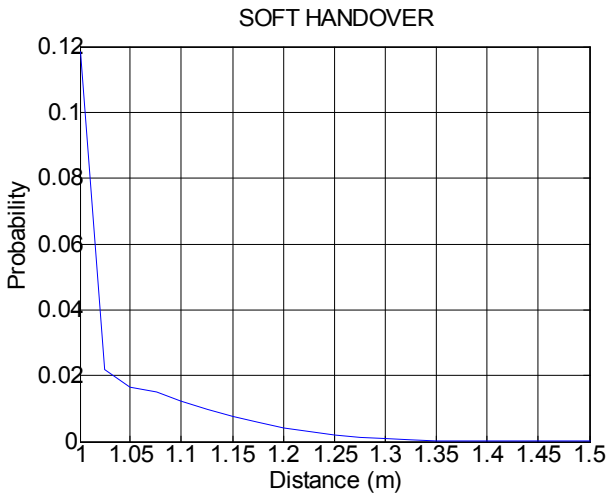

Fig. 10 Soft HO.

The propagation model can be probed changing the power of the link distance. In the Table 2 this parameter is used for low, medium and high log-normal distributed shadowing. The experimental results indicate the values listed in this table.

σ	μ=2	μ=4	μ=7
0	0.7278	0.4009	0.2992
1	0.7474	0.4116	0.3073
2	0.8093	0.4457	0.3327
3	0.9240	0.5089	0.3799
4	1.1124	0.6126	0.4573
5	1.4121	0.7777	0.5806
6	1.8902	1.0410	0.7771
7	2.6679	1.4694	1.0969
8	3.9707	2.1869	1.6325
9	6.2314	3.4320	2.5619
10	10.3117	5.6792	4.2395
11	17.9929	9.9097	7.3975
12	33.1054	18.2330	13.6108

Table. 2 Standard Deviation for several propagation models.

The density of users is determined by number of users in the cell and the geometry of the cell. In this paper, hexagon cells are considered, see equation 4.

$$k = \frac{2k}{3\sqrt{3}} \qquad (4)$$

The presence of shadowing means that users may not necessarily operate to the nearest base station, but to the base station for which path loss is minimal.

As a result, the interference from other-cell users is calculated by equation 5.

$$I_{\bar{S}_0} = E\iint_{\bar{S}_0}\left[\frac{r_1^{\mu}(x,y)10^{\zeta_1/10}}{r_0^{\mu}(x,y)10^{\zeta_0/10}}\right]kdA(x,y) \qquad (5)$$

And finally, the relative other cell interference factor can be computed by equation 6.

$$f = \frac{I_{\bar{S}_0}}{k_u} = e^{b^2(\beta\sigma)^2}\left[\frac{2}{3\sqrt{3}}\iint_{\bar{S}_0} R_1^{\mu}(x,y)dA(x,y)\right] \qquad (6)$$

The equation 6 involves numerical integration and a specific geometry restrictions. In this work, the following assumptions are considered in the geometry of the cell: the size of the cell is a constant and it is normalized.

In Table 3 the comparison for common frequency reuse schemes is given. The standard deviation of the log-normal.

σ	k=2	k=4	k=7	k=12	k=21
0	0.2992	0.0398	0.0025	0.0011	0.0001
1	0.3073	0.0408	0.0025	0.0011	0.0001
2	0.3327	0.0442	0.0027	0.0012	0.0001
3	0.3799	0.0505	0.0031	0.0014	0.0001
4	0.4573	0.0608	0.0037	0.0017	0.0002
5	0.5806	0.0771	0.0048	0.0021	0.0002
6	0.7771	0.1032	0.0064	0.0029	0.0003
7	1.0969	0.1457	0.0090	0.0040	0.0004
8	1.6325	0.2169	0.0134	0.0060	0.0006
9	2.5619	0.3403	0.0210	0.0094	0.0010
10	4.2395	0.5632	0.0347	0.0156	0.0016
11	7.3975	0.9827	0.0606	0.0273	0.0028
12	13.6108	1.8080	0.1116	0.0502	0.0051

Table. 3 Standard Deviation for some frequency reuse schemes

The algorithm implemented evaluates the hard and soft handover for inter-cell interference. The selection of the cluster considers the following frequency reuse schemes: two, four, seven, twelve and twenty-one, regular and normalized cells.

The calculation of the distance between the terminal equipment is particularly important, because it determines the power level of the intentional interference.

In the Figures 11 and 12 the two main routines of the model simulation are plotted.

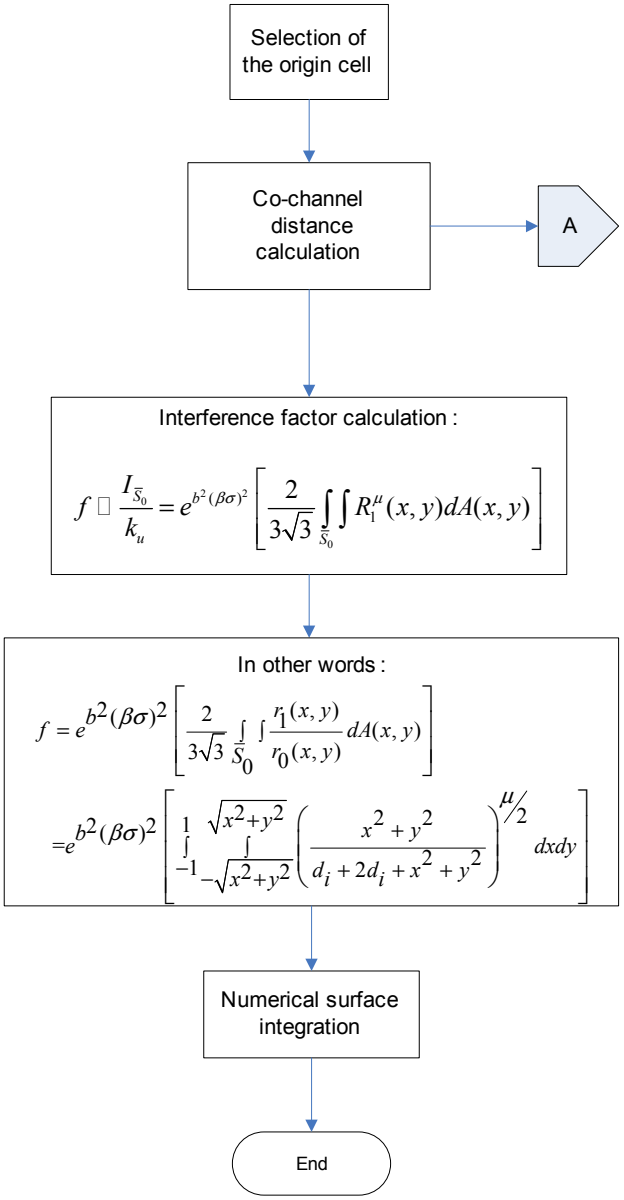

Fig. 11 Algorithm implemented.

The complementary procedure of the proposed algorithm involves the computation of the distance to several base stations. This bases stations are transmitting at the same carrier frequency.

The co-channel interference level is decreased for a large cluster, because the number of interfering base stations do not compensate the attenuation of the signal.

The interference factor requires the use of numerical double-integration. This step involves a large computation time. The distance calculation also increases the number of operations, because the it is necessary to consider all the base stations in the cluster.

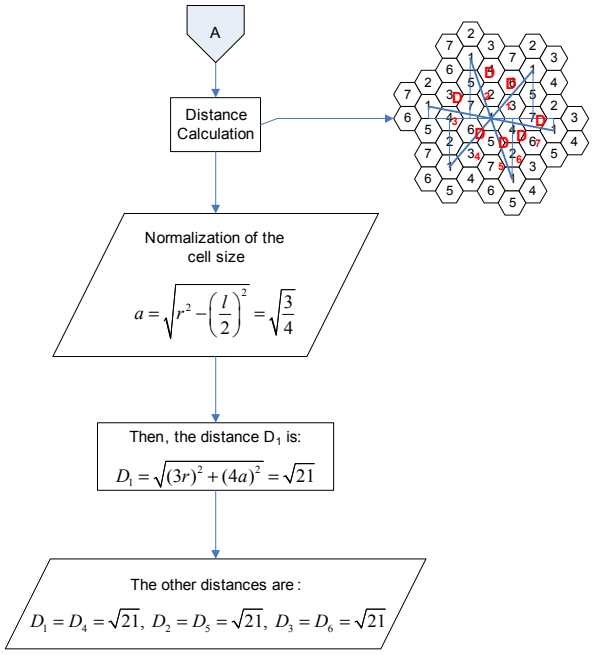

Fig. 12 Distance calculation.

In order to illustrate this algorithm, the distance calculation is shown in Figure 13, for the four-cell frequency reuse.

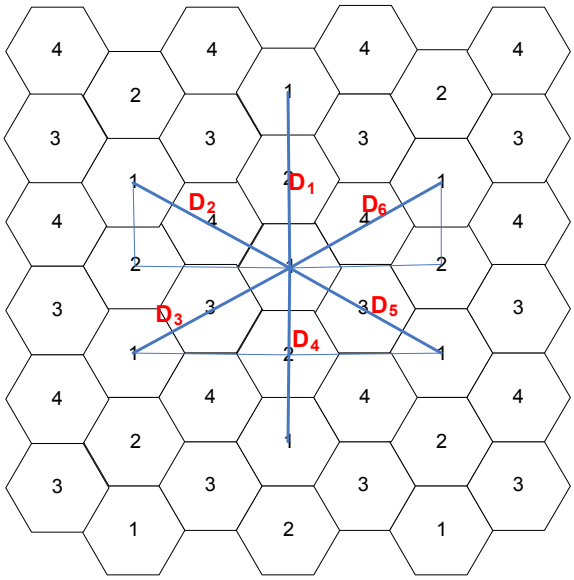

Fig. 13 Four cell frequency reuse.

In the Figure 14 the distance calculation of the seven cells frequency reuse technique is drawn.

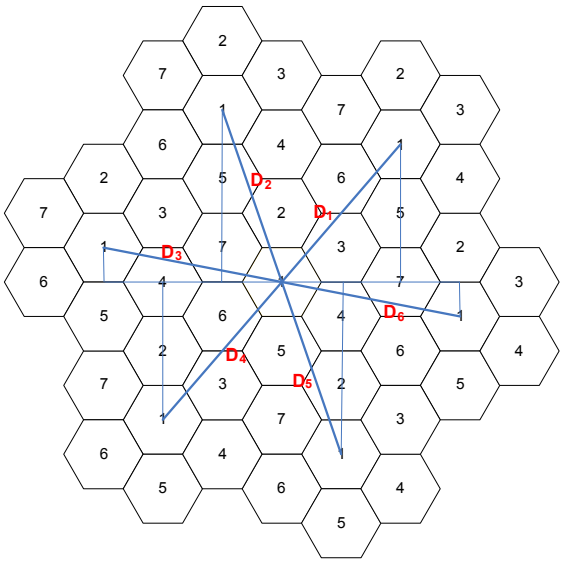

Fig. 14 Seven cells cluster

Similarly, in the Figure 15 the distance calculation of the twelve cells frequency reuse technique is plotted.

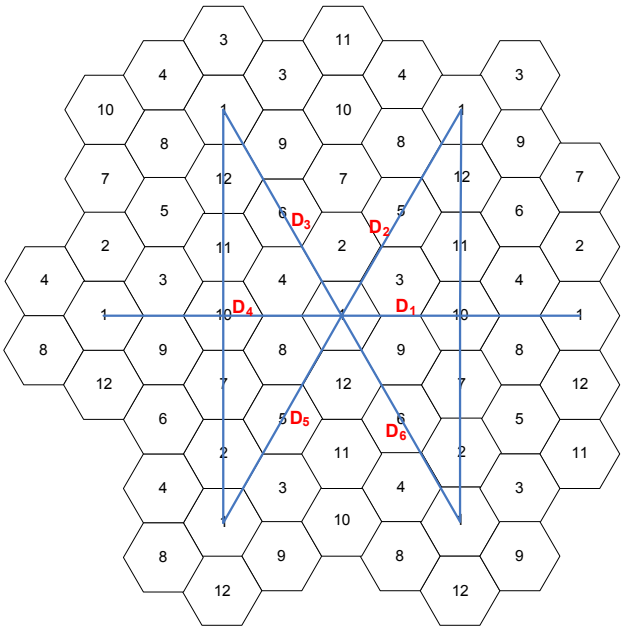

Fig. 15 Twelve cell frequency reuse.

Finally, in the Figure 16 the distance calculation of the twenty-one cells frequency reuse technique is drawn.

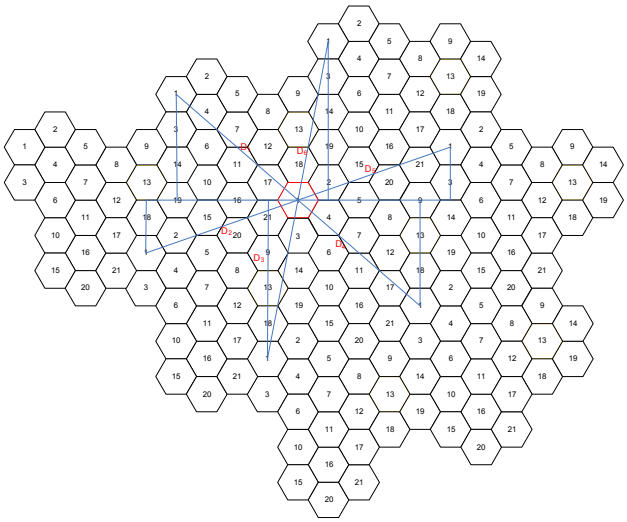

Fig. 16 Twenty one cell frequency reuse.

This procedure can be extended to other sizes of cluster. In a non-regular set of cell, the radius of them could be not a constant.

The computation time depends on the cluster size, because the number of interfering base station may increase.

The consideration of short-term fluctuations for fast Rayleigh fadind may also increase the computation time.

5 Results

The simulation parameters are defined in equation 7, and the normalized distances from other interfering cells were found for 2, 4, 7 and 12, frequency reuse schemes.

The equation 7 determines the most practical values of the model. The results presented in this section has been calculated in this conditions.

$$d = 2\,,\ \beta = \ln(10)/10\,,\ b = 1/\sqrt{2}\,,\ \mu = 5 \qquad (7)$$

The main results obtained were the other-cell interference factor as a function of the standard deviation of the log-normal shadowing. The same frequency reuse schemes used in the section presented before, was employed to illustrate the model simulations.

The Figure 17 the normalized distances from other cells is given for a two cell frequency reuse scheme.

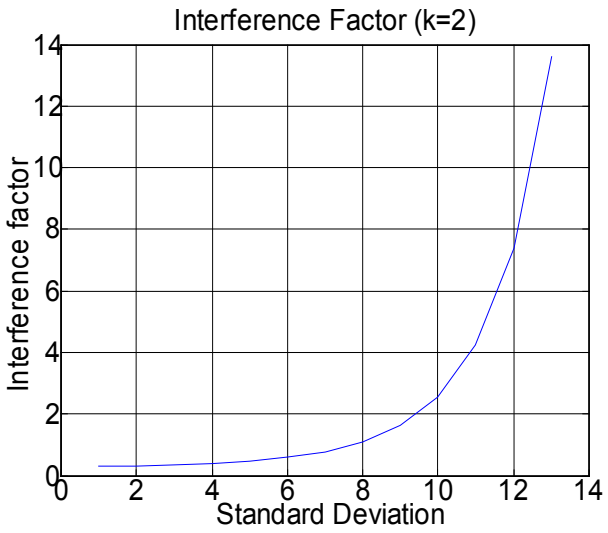

Fig. 17 Two cell frequency reuse scheme.

From Figures 18 to 21 the Other-Cell Interference factor is illustrated for the most practical frequency reuse schemes.

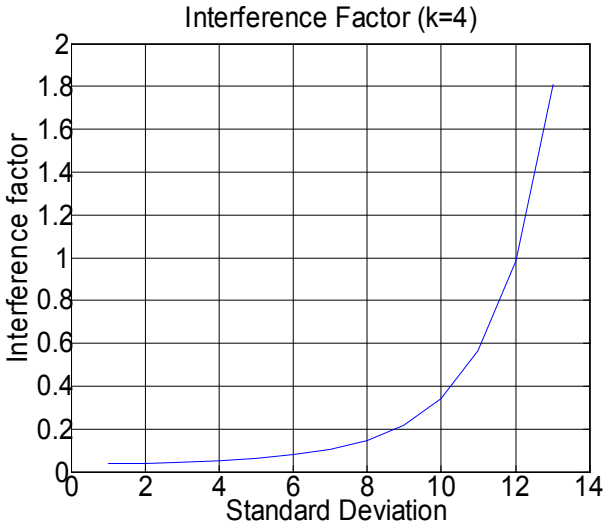

Fig. 18 Four cell frequency reuse scheme

It is important to highlight the vertical axis in these figures, the regular hexagon size of the cells narrows down the Other-Cell interference factor, because the normalized distance are notably increased.

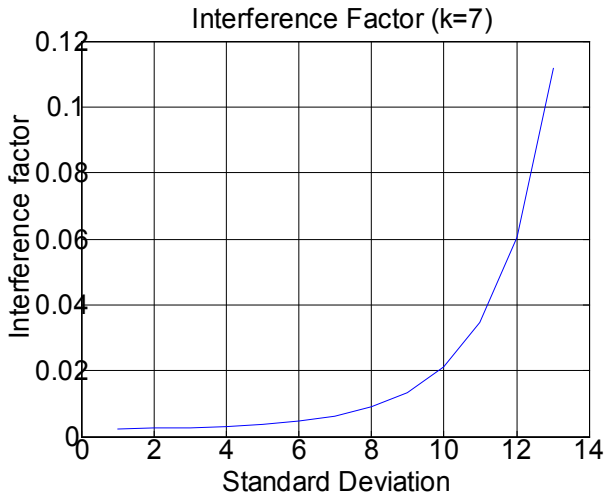

Fig. 19 Seven frequency reuse scheme

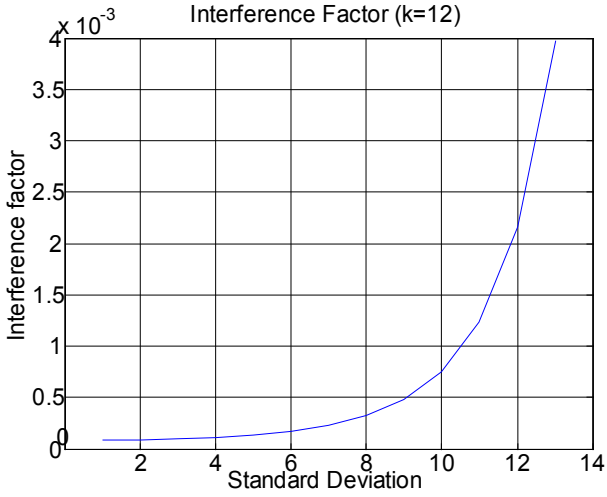

Fig. 20 Twelve frequency reuse scheme.

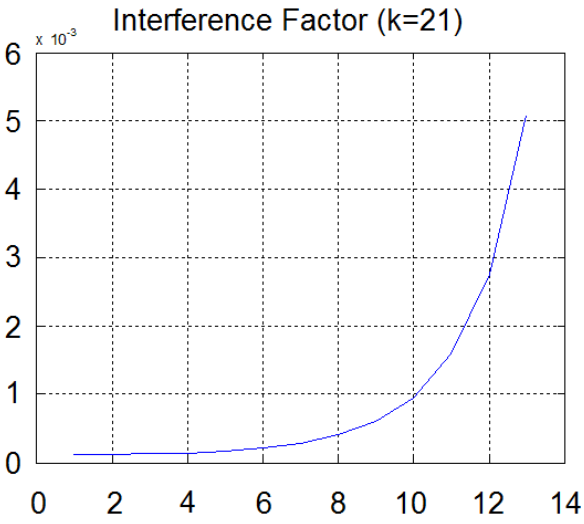

Fig. 21 Twenty-one frequency reuse scheme.

The calculation of the other cell interference factor allows to compare it with the signal power level, and then evaluate the performance of the system.

6 Conclusions

The outage probability in Hard HO is greater than Soft HO, but it is necessary to calculate the intra-cell interference, because it can be increased.

It is necessary to consider that the Soft HO requires more resources to be in operation. The intra-cell interference may be increased.

The Softer HO has not be considered in this paper, but the same procedure can be applied.

A large cell frequency reuse scheme has a low Other-Cell interference factor, because the normalized distance is normally less than other. It is important to find an intermediate situation.

This work is currently enhanced with other frequency reuse schemes and, the calculation of interference to signal ratio allow us to evaluate the bit rate of the system. In addition to this, the size and the form of the cells could be a variable in future simulations.

The algorithm presented was implemented in Matlab, but the computation time is quite large, other methods are being used to reduce this problem for future works [6].

It is important to emphasize that the non-linear effects in the power amplifiers are not considered in this article. A complete analysis of this impairment is detailed in [7].

In the same way the outage probability is very important to determine the availability of the system, and the traffic considerations could be enhance the model.

References:

[1] A. J. Viterbi, A. M. Viterbi, K. S. Gilhousen, E. Zehavi, " Soft Handoff Extends CDMA Cell Coverage and Increases Reverse Link Capacity", *IEEE Communications*, Vol. 12, No.8, pp 1281-1288, October 1994.

[2] Jijun Luo, Markus Dillinger, Egon Schulz, Zaher Dawy, "Optimal Timer Settingd for the Soft Handover Algorithm in WCDMA".

[3] H. Holma, A. Toskala, "WCDMA for UMTS, Radio Access for third Generation Mobile Communications." Third Edition, 2004, Ed. Wiley, 2000, pp. 52-60,.75-93, pp.245-260.

[4] J. Laiho, A. Wacker, T. Novosad. "Radio Network Planning and Optimization for UMTS", Second Edition, 2006, Ed. John Wiley & Sons Ltd, pp 27-28, pp. 211-224.

[5] Leon W. Couch, "Digital and Analog Communications Systems", Prentice Hall, Fifth Edition, 1997.

[6] Athanaileas, T.E., Gkonis, P.K., Athanasiadou, G.E., Tsoulos, G.V., Kaklamani, D.L., "Implementation and Evaluation of a Web-Based Grid-Enabled Environment for WCDMA Multibeam System Simulations", *IEEE Antennas and Propagation Magazine*, Vol. 50, No. 3, June 2008, pp.195-204.

[7] Yong-Sub L., Mun-Woo L., Yoon-Ha J., "Highly Linear Power Tracking Doherty Amplifierfor WCDMA Repeater Applications", *Microwave and Wireless Components Letters*, Vol. 18, No. 7, July 2008, pp. 485-487.

[8] Chi-Fang L., Yuan-Sun C., Jan-Shin H., Wern-Ho S., "Cell Search in WCDMA Under Large-Frequency and Clock Errors: Algorithms to Hardware Implementation", *IEEE Transactions on Circuits and Systems I: Regular Papers*, Vol. 55, No. 2, March 2008, pp.659-671.

[9] Fu, H., Kim, D.I., "Scheduling performance in downlink WCDMA networks with AMC and fast cell selection", *IEEE Transactions on Wireless Communications*, Vol. 7, No. 7, July 2008, pp. 2580–2591.

[10] Augustin, G., Bybi, P.C., Sarin, V.P., Mohanan, P., Aanandan, C.K., Vasudevan, K., "A Compact Dual-Band Planar Antenna for DCS-1900/PCS/PHS, WCDMA/IMT-2000, and WLAN Applications", *IEEE Antennas and Wireless Propagation Letters*, Vol. 7, 2008, pp. 108–111.

[11] Hyejeong S., Huijung K., Kichon H., Jinsung C., Changjoon P., Bumman K., "A Sub-2 dB NF Dual-Band CMOS LNA for CDMA/WCDMA Applications", *IEEE Microwave and Wireless Components Letters*, Vol. 18, No. 3, March 2008, pp. 212-214.

[12] Martel, P., Lossois, G., Danchesi, C., Brunei, D., Noel, L., "Experimental investigations on BER degradations due to analogue channel filtering in zero-IF receivers for FDD WCDMA", *Electronics Letters*, Vol. 44, No. 2, January, 2008, pp. 138–139.

[13] Bello, P. A., "Caracterization of randomly time – variant linear channels", *IEEE Transactions on Communications Systems*, Vol. CS-11, No. 4, 1963, pp. 360-393.

[14] Jakes, W. C., "Microwave Mobile Communications", Addison-Wiley, 1994.
[15] Parson, J. D., Bajwa, A. S., "Wide-Band caracterization of fading mobile radio channels", *Proceedings of the IEEE*, Vol. 129, No. 2, pp. 95-101, 1982.